



# Improved locations for teleseismic earthquakes using surface waves

Michael Howe & Göran Ekström

Lamont-Doherty Earth Observatory, Columbia University

PI: Göran Ekström, ekstrom@ldeo.columbia.edu (howe@ldeo.columbia.edu)

Consortium for Verification Technology (CVT)

Lamont-Doherty Earth Observatory  
COLUMBIA UNIVERSITY | EARTH INSTITUTE

## Abstract

Current earthquake-location capabilities provide no better than 25-km precision in remote areas, which is insufficient for many tectonic investigations. Differential body-wave relocation schemes offer limited improvements, particularly in the oceans where P waves are often poorly observed. Surface waves, with their slow horizontal propagation speeds and high signal strength even at teleseismic distances, contain information on earthquake location that can improve epicenter determinations. Earlier work by other authors has demonstrated the possibility of precise relative location by cross-correlation of Rayleigh waves for pairs of earthquakes with the same focal mechanism and depth, and Cleveland and Ammon (2013) have recently demonstrated success with this approach for multiple events with similar mechanisms and a double-difference relocation method. We extend earlier approaches to improve relative locations for earthquakes with arbitrary focal mechanisms. We correct inter-event cross-correlation functions of Love and Rayleigh surface-wave signals for differences in focal mechanisms and depths before calculating cross-correlation delay times and relative locations. Experiments on full synthetic seismograms indicate that the algorithm results in improved locations in the presence of realistic uncertainties in earthquake focal depths and mechanisms. We present results from the synthetic experiments and applications to real data, using earthquakes from the Global CMT catalog representing different tectonic environments.

## Introduction

Surface waves are both the largest and the slowest-propagating signals recorded on a seismogram. Arrival-time differences for different earthquakes with relatively small inter-event distances give information about the relative location of those earthquakes. This measure of relative earthquake location, when combined with many other similar measurements for nearby earthquakes, can substantially improve location estimates and reduce location uncertainties with respect to traditional single-event location estimates.

A demonstration of the effectiveness of surface-wave relocation can be seen in Figure 1. Here, earthquake locations and mechanisms are plotted before (top) and after (bottom) surface wave relocation. The focusing of earthquakes on linear features is consistent with the pattern of seismicity anticipated from plate tectonics. These earthquakes, in the Eitanin Fracture Zone in the southern Pacific Ocean, are well-suited to this method since they are predominantly strike-slip and normal-faulting earthquakes.

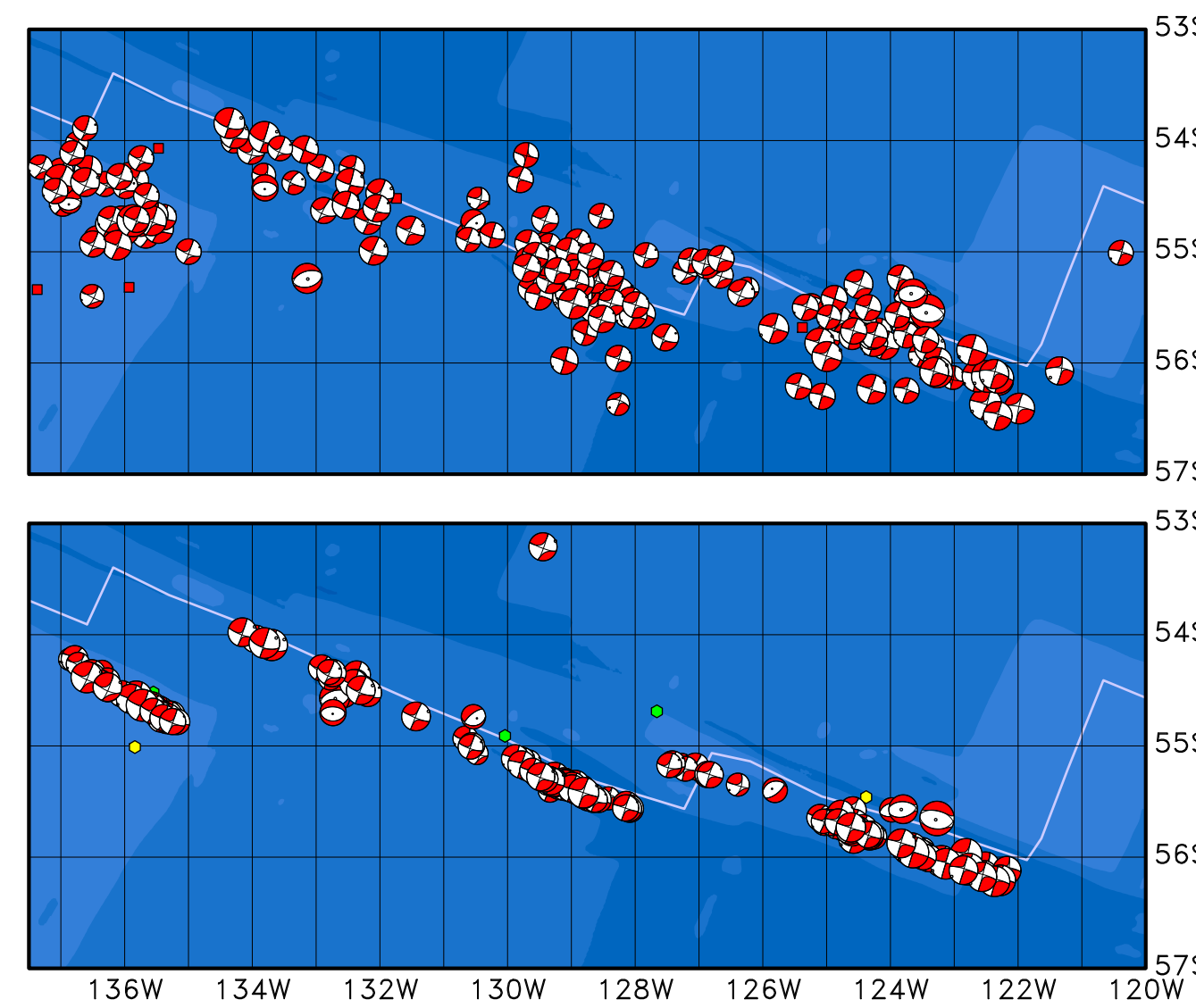


**Figure 1:** Eitanin Fracture Zone relocations. Significant location improvement when comparing before (top) and after (bottom) surface wave relocations. The gray lines are plate boundaries which, as can be seen by the relocated earthquakes, are not entirely correct.

The type of earthquake source is very important to this type of relocation technique, since some earthquake geometries generate phase shifts in the recorded seismograms that can mimic a location shift. The corrections required to account for arbitrary earthquake geometries in the application of the surface-wave relocation is the focus of the remainder of this poster.

## Theory

The measurement to determine the calculated inter-event distance and azimuth is the time-lag of the cross-correlation between the recorded waveforms of two events within a prescribed inter-event distance. If the effect of the receiver is removed, each waveform can be expressed as a convolution of the effects of the path of propagation (Green Function) and the effects of the source. In the frequency domain, this is a product of those two terms, as shown in Equations 1 and 2.

$$u^A(\omega) = G^A(\omega)S^A(\omega) \quad (1)$$

$$u^B(\omega) = G^B(\omega)S^B(\omega) \quad (2)$$

The cross-correlation of these two waveforms is (again in the frequency domain) the complex conjugate of waveform A multiplied by waveform B, as in Equation 3.

$$C^{AB}(\omega) = G^A G^{B*} S^A S^{B*} \\ = G^A G^{B*} \cdot [R^A R^{B*} - J^A J^{B*} + i(R^A J^{B*} - J^A R^{B*})] \quad (3)$$

The cross-correlation function in Equation 3 will include any phase shift from the effects of the earthquake sources if the imaginary component (J) of the radiation patterns is non-zero. This is the case if the component of the source mechanism that represents slip on a vertical fault (vertical dip-slip) is large compared to the other components. In order to correct for this effect, I first need to calculate the R and J for each earthquake, and then (as shown in Equation 4) divide the cross-correlation by the source effects of the two earthquakes. An example of what this effect looks like (for both Love waves and Rayleigh waves) for two example earthquakes is shown in Figure 2.

$$C_{corr}^{AB}(\omega) = \frac{C^{AB}(\omega)}{S^A S^{B*}} \quad (4)$$

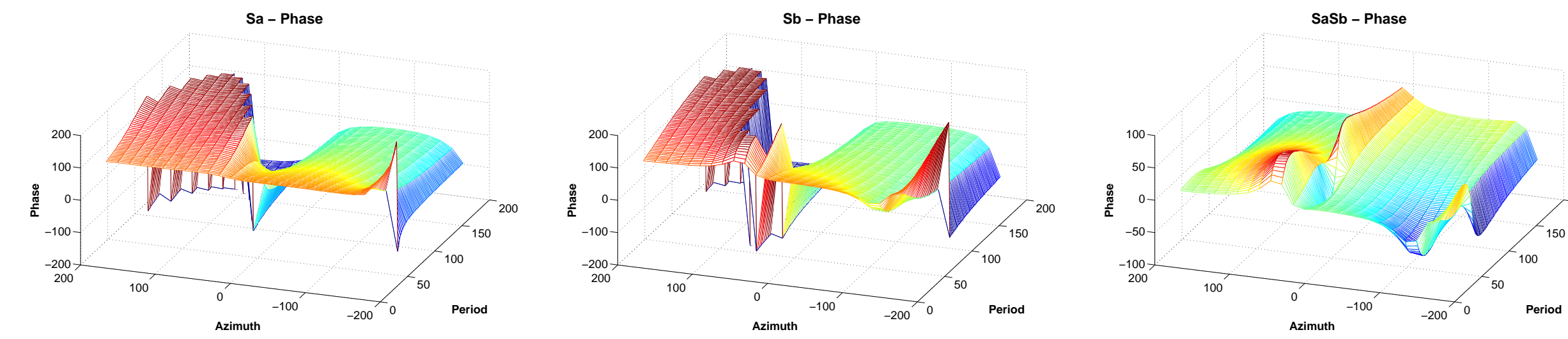


**Figure 2:** Phase of two reverse-faulting earthquakes with a vertical dip-slip component and slightly rotated relative strikes: Strike/Dip/Rake = 189/20/94 (left) 228/17/124 (middle). The combined phase vs. frequency and azimuth is shown in the right panel.

## Synthetics - Simulated Subduction Zone

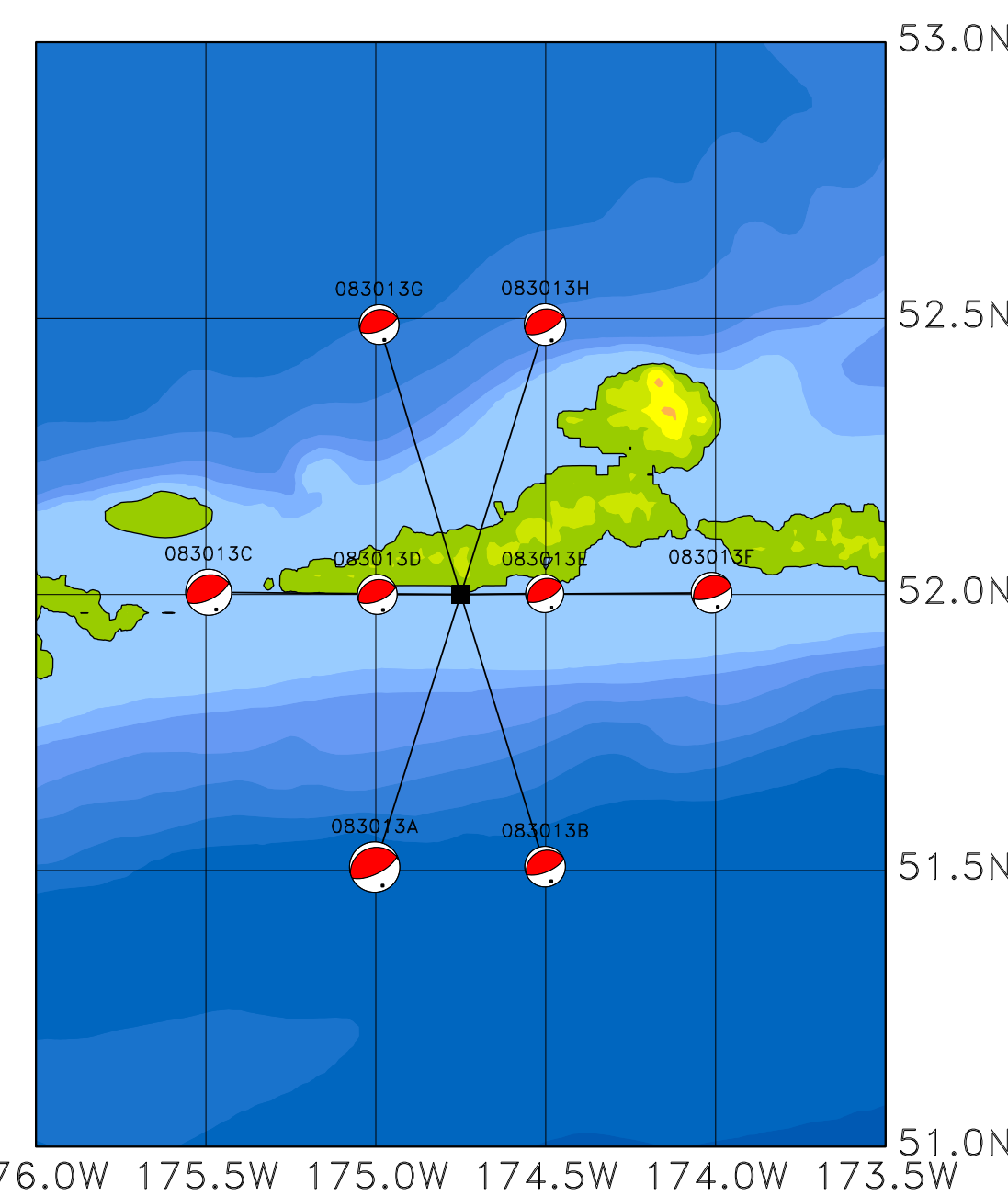


**Figure 3:** Synthetic earthquake relocations. The initial locations for all events was in the very center of the cluster.

Before applying the source correction to data recorded for real earthquakes, we tested the method on synthetic data. Since this correction will be most useful for events with large relative phase delays we used synthetic earthquakes geometries that have relatively large imaginary components in their surface wave radiation patterns. A geologic setting where this applies is a subduction zone, so we simulated a subduction zone with appropriate source mechanisms and source depths. We generated synthetic seismograms for a range of azimuths using moment tensors from real earthquakes in the Aleutian Islands in Alaska. The locations and depths of the synthetic events are prescribed to be at 8 distributed locations at 3 different depths. The relocated events are shown in Figure 3. The same locations are shown in profile in the bottom of Figure 4. The top of Figure 4 is a plot of the RMS misfit of the relocations with correction against the relocations without correction. There is significant reduction of the misfit for the corrected relocations.

To the right, Figure 5 shows two example of the observed cross-correlated time-lags. Observations with and without corrections are plotted along with the relocation prediction.

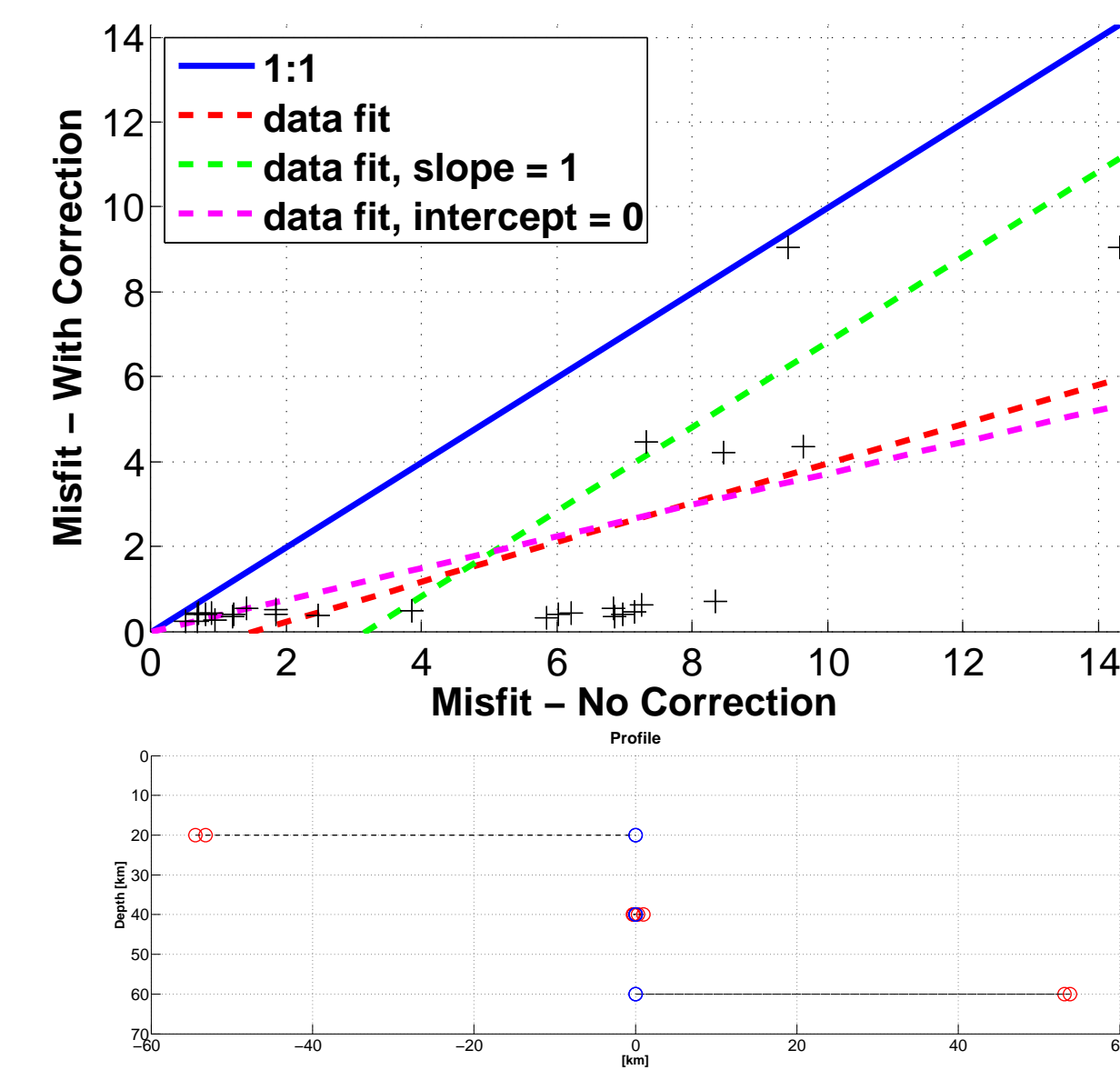


**Figure 4:** (Top) Misfits plotted against each other for relocations before and after correction. The blue line illustrates where a point would be plotted with no change in misfit. (Bottom) Locations shown in profile for the relocations with corrections. Note that the initial locations are all in the middle and move to the true location appropriate for the angle of the subducting slab.

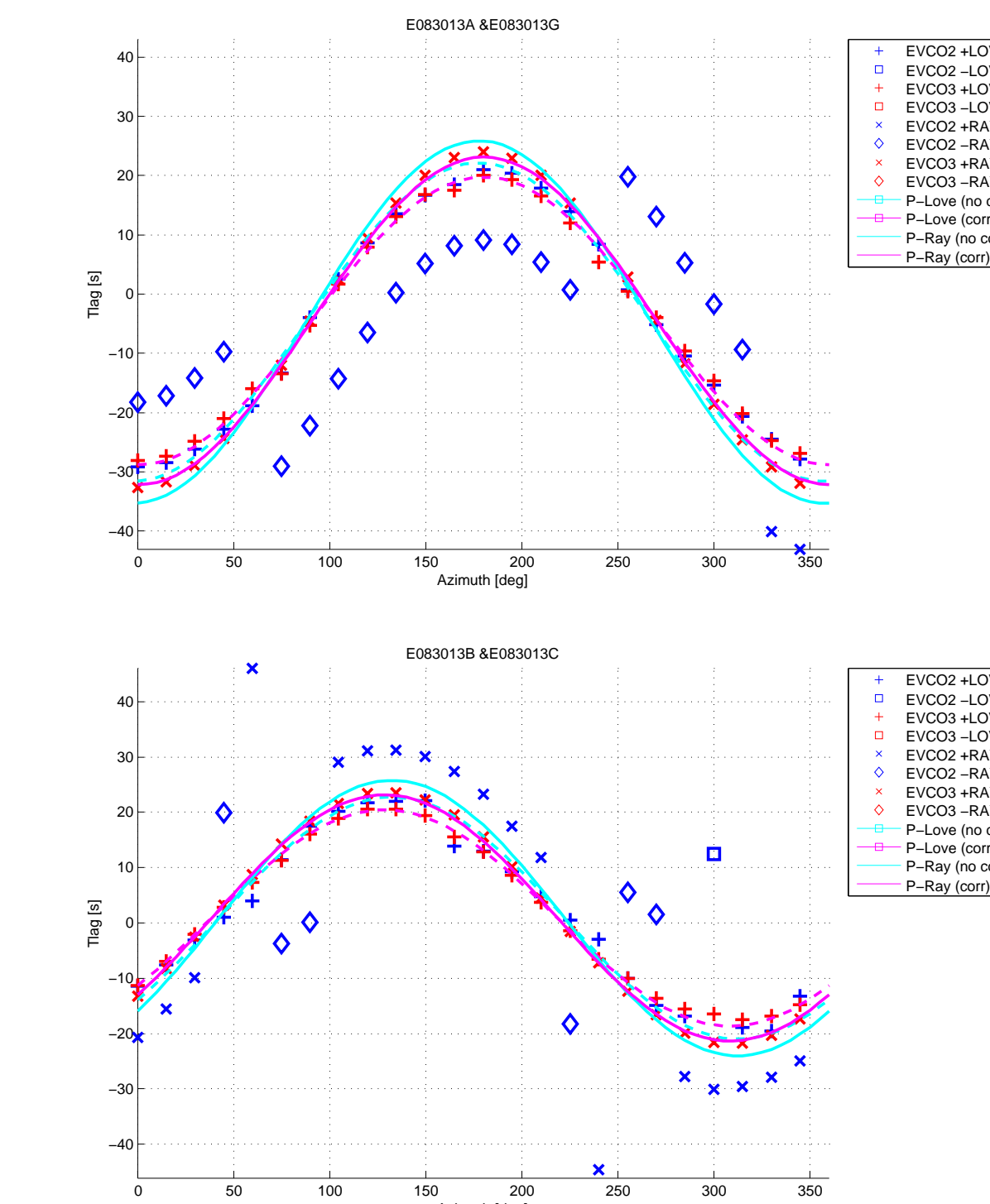


**Figure 5:** Example of two inter-event pair cross-correlations. Shown are corrected (red) and uncorrected (blue) time-lag measurements, as well as the prediction from the relocation (magenta). The data are further subdivided into Love waves and Rayleigh waves as indicated by the legend.

## Real Data - Aleutians

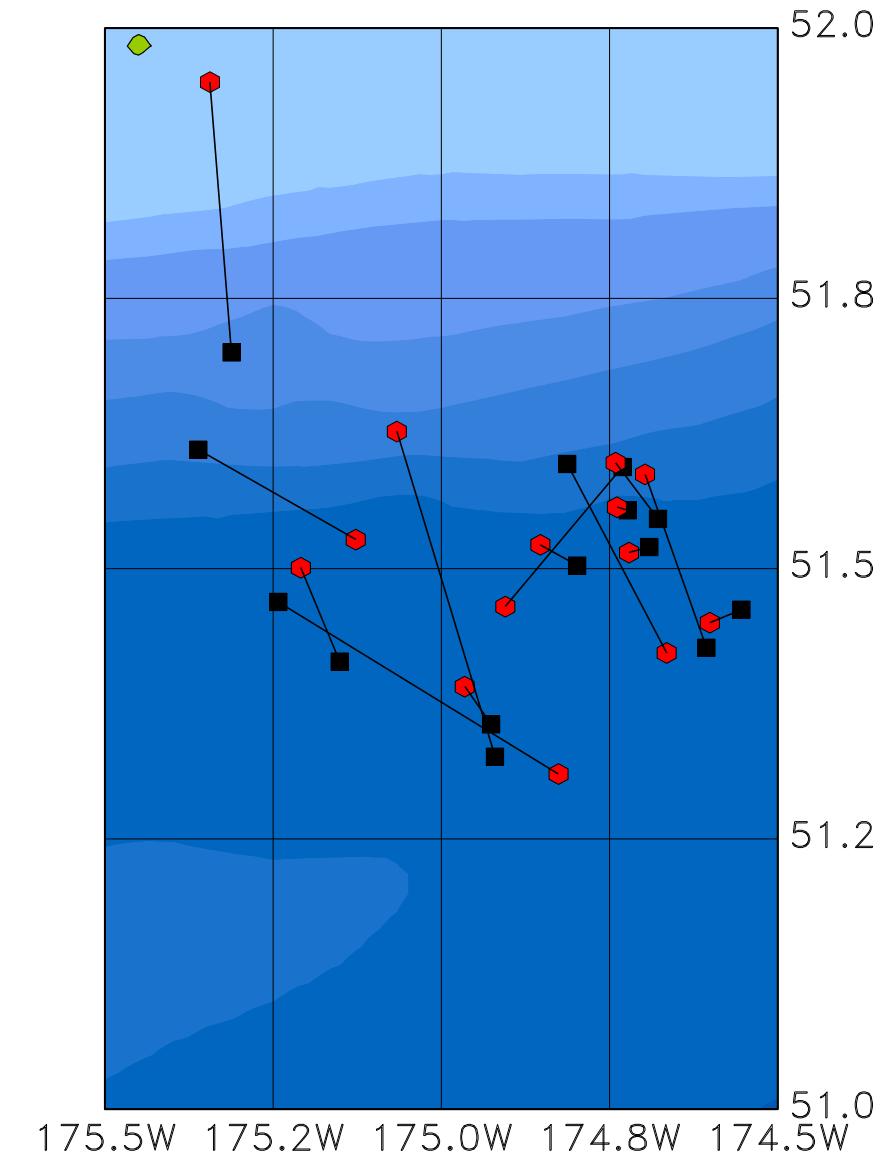


**Figure 6:** Synthetic earthquake relocations. The initial locations for all events are the black circles and they are connect by a black line to the new locations, which are plotted as red circles.

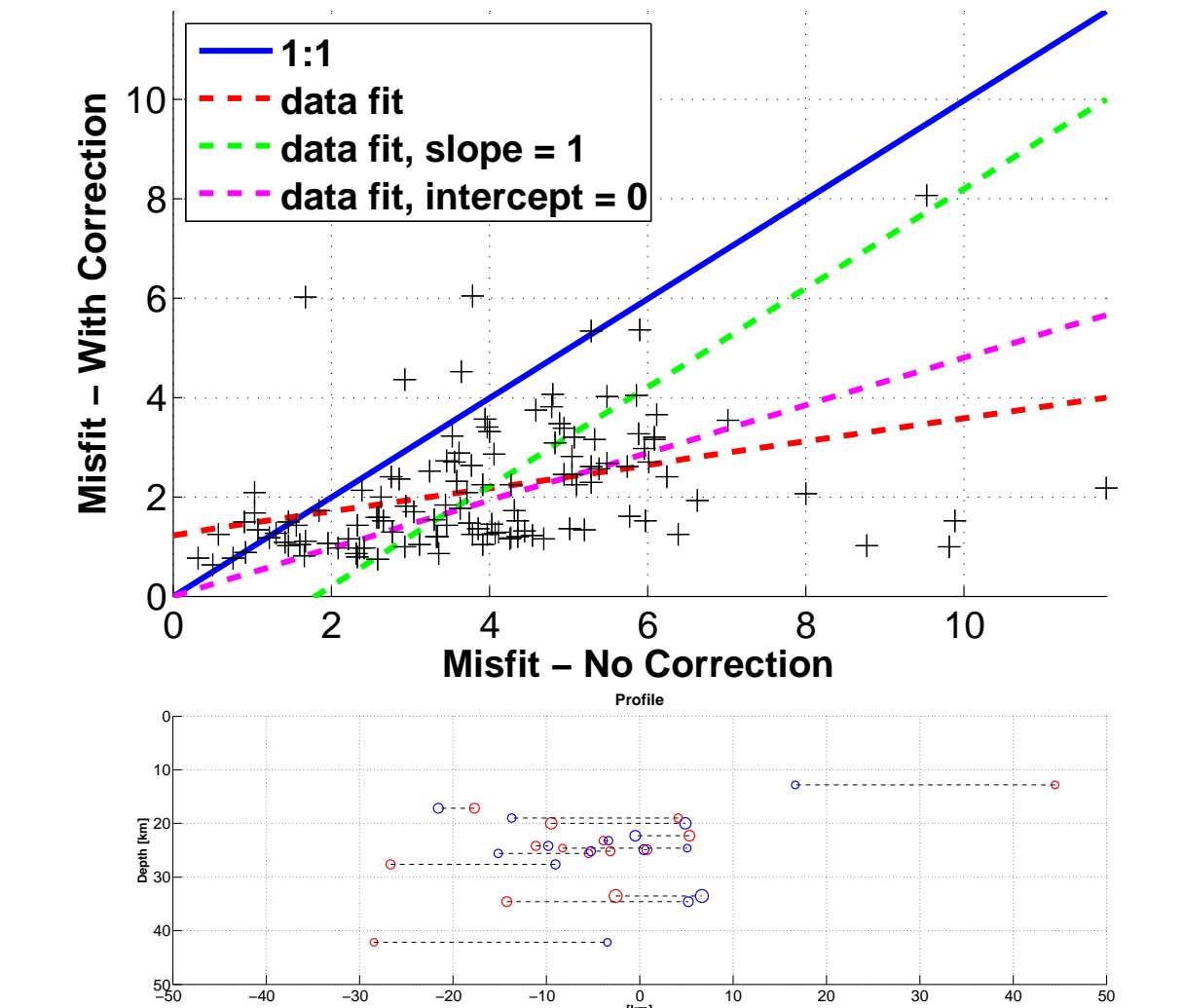


**Figure 7:** (Top) Misfits plotted against each other for relocations before and after correction. The blue line illustrates where a point would be plotted with no change in misfit. (Bottom) Locations shown in profile for the relocations with corrections.

Building upon what we learned using synthetic earthquakes, we apply our source corrections and relocation algorithm to real earthquakes. A sequence of 32 earthquakes from August to November of 2013 in the Aleutian Islands was selected for analysis. Two period bands were initially used to filter the data, and the best results were achieved with long-period (40s - 80s), band-passed data. The relocations (in map-view and in profile) along with an RMS misfit analysis are shown in Figures 6 & 7. Again, there is significant misfit reduction after the source corrections are made.

To the right, Figure 8 shows examples of cross-correlation delays of 2 inter-event pairs. It is evident that there are significant differences to observations with and without source corrections. It is notable that the predictions do not quite reach the observations in these two examples. We do not expect a perfect fit since the relocation is calculated using residuals for all 32 events simultaneously. The best fit for all the data simultaneously is not necessarily the best for an individual event pair.

The results from applying our method to real are encouraging. Further development of this method will continue for this region as well as other appropriate regions to optimize the technique for accuracy and efficiency.

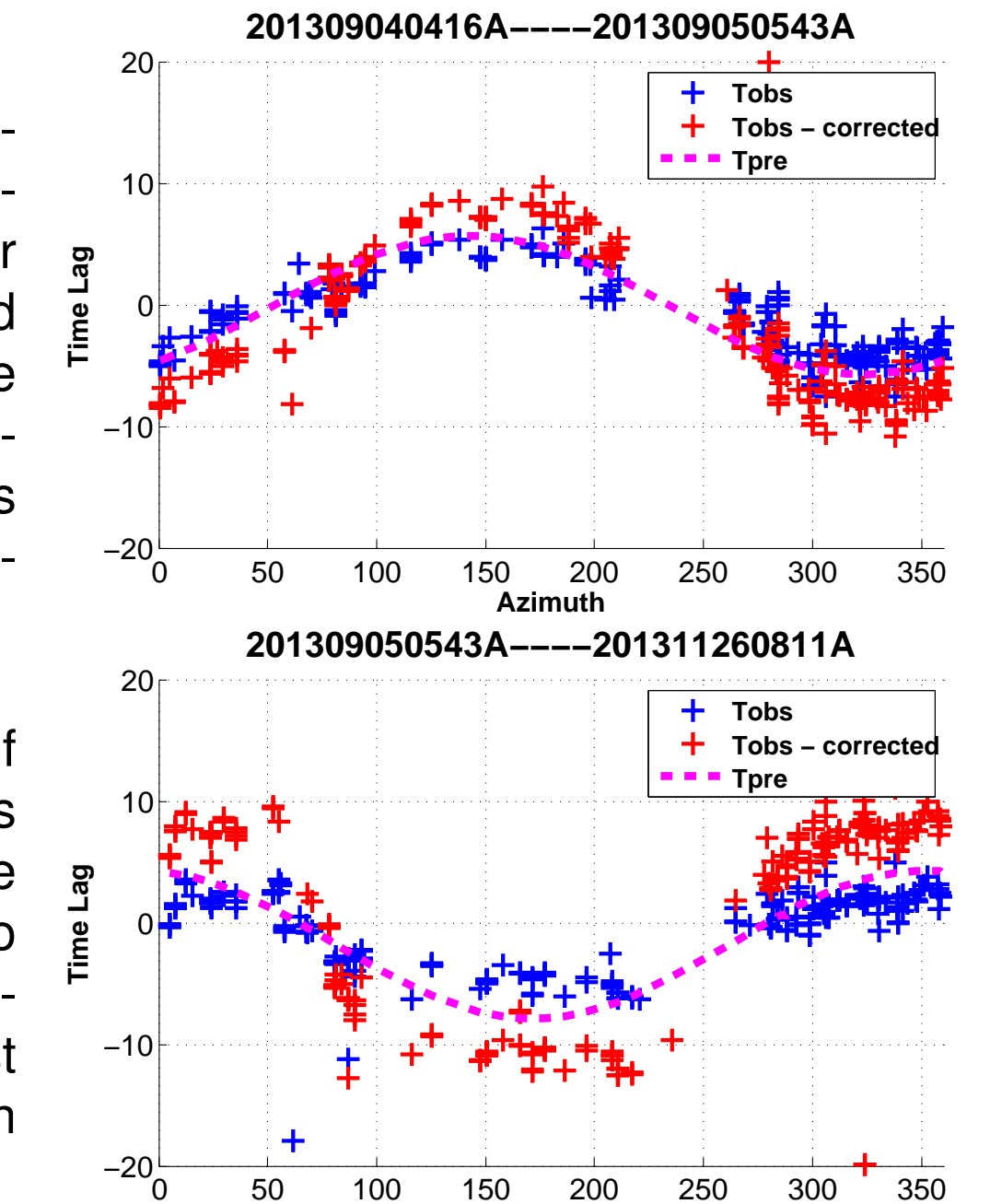


**Figure 8:** Example of two inter-event pair cross-correlations. Show are correct (red) and uncorrected (blue) time-lag measurements, as well as the prediction from the relocation (magenta)

## Forthcoming Research

We plan to further develop the method presented here to improve earthquake locations routinely and on a global scale.

Building upon this work, we plan to investigate the generation of long-period surface waves by underground nuclear explosions, including the non-isotropic radiation that is attributed to the release of tectonic stresses in the host rock.

## Acknowledgements

This work was funded in-part by the Consortium for Verification Technology under Department of Energy National Nuclear Security Administration award number DE-NA0002534. The data used was obtained from the Global Seismographic Network through the United States Geological Survey and the Incorporated Research Institutions for Seismology.